

Keage Laboratory of Nuclear Science Decennial Report 1978~1988

Hidekuni TAKEKOSHI

Received July 6, 1990

The activities of the Keage Laboratory of Nuclear Science done in the period from 1978 to 1988 are reviewed. However in 1987 the cyclotron at the Keage Laboratory was shut down, so that the report was mentioned mainly about the experiments done with this cyclotron.

INTRODUCTION

The foremost decennial report (from 1967 to 1977), was written by professor Takuji Yanabu¹⁾ in 1977. Since then two laboratories, Laboratory of Nuclear Reaction and Nuclear Science Research Facility, of the Institute for Chemical Research at Keage, were amalgamated as a new laboratory of Nuclear Science Facility in 1986 and the cyclotron was shut down in 1987. A new proton linac project started in 1986 and a new building for the proton linac was built at Uji campus area in 1988. The old building at Keage was closed in 1990. As for the staff, the former chief of the Keage laboratory, professor Takuji Yanabu retired in 1982 under an age limit, and Makoto Inoue was appointed as the new professor in 1985. The Kyoto University Cyclotrons²⁾ was improved for acceleration of ³He ions and heavy ions besides acceleration of protons, deuterons and alpha particles in 1970–1973³⁾. However, taking out of the ³He ion beam or the heavy ion beam externally from the cyclotron was not an easy task, so the experiments were usually done with the external beams of protons, deuterons or alpha particles. In 1976 a cyclotron of the Nuclear Physics Research Centre at Osaka University was in operation, since then the nuclear physics experiments by the staff of Keage laboratory were mainly done with the Osaka University Cyclotron. The activities about the accelerator physics and the nuclear physics done by the staff in this period will be reported in future.

Therefore new uses of Keage cyclotron other than the nuclear physics were mentioned here. One of them was the material analysis using the proton beam or the alpha beam. The methods developed were the Rutherford back scattering (RBS) and the particle induced X-ray emission (PIXE). The sensitivity of these were extremely high and a very small amount of sample were needed.

The other was about the radiobiology. The basic research about the cancer therapy with fast neutrons was studied. In the experiments the relative biological effect (RBE) values of fast neutrons produced with the cyclotron were measured. And chromosome aberrations between cells induced by protons and alpha particles, and a

竹腰秀邦: Nuclear Science Reserch Facility, Institute for Chemical Research, Kyoto University, Uji, Kyoto-fu 611, Japan.



Photo. 1. The first 100cm cyclotron project was planned by the late professor Bunssaku Arakatsu in 1942. However, this cyclotron which was still under construction was all destroyed by the occupation forces after the end of the World War II in 1945. Photo shows the magnet pole and yoke of the cyclotron. First row from right to left Prof. Kimura and Mr. Hori, second row Prof. Arakatsu, Mr. Uji and Prof. Uemura.

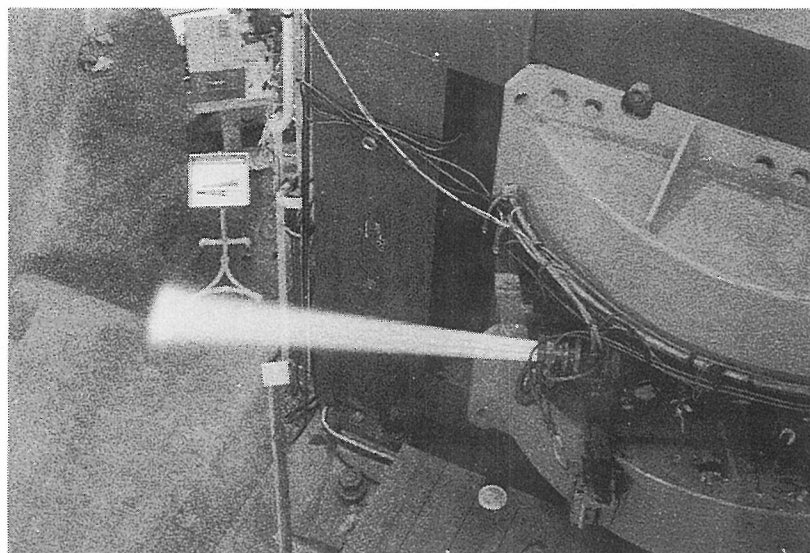


Photo. 2. External proton beam. The second 105cm cyclotron was completed under the direction of Prof. Kiichi Kimura in 1955, and was operated in 10 years period. And then the cyclotron was improved by Prof. Uemura in 1970-1973, since then the cyclotron had been in operation until the shut down at 1987.

dose-response relation of dicentric yield were studied. Outlines of those studies are as followings.

MATERIAL ANALYSIS

1. RBS analysis

The Rutherford back scattering method, RBS, is a useful method to determine the composition variation and the impurity distribution as a function of depth below the surface of sample. The energies of nuclear scattered particles by sample nuclei are measured, and the information about the elemental composition near the sample surface can be obtained. The energies of projectile ions commonly used in the RBS method are usually under the coulomb-barrier energy of the nuclear interaction, i. e., the energy of protons and that of alpha particles are lower than 3 MeV and 5 MeV respectively. The information about the sample depth of a few micron with the position sensitivity of the order of 100 angstroms can be obtained.

The analysis of the distributions of light elements, such as hydrogen, carbon, nitrogen and also heavy elements, in the sample surface of hundreds angstrom thickness were tried with projectile ions of higher energies, 6.9 MeV protons and 27.6 MeV alpha particles from the Kyoto University Cyclotron⁴). The numbers of samples were mounted on a long aluminum holder placed at a center of a big vacuum chamber. The holder could slide up and down and also could rotate. The collimated beams of 6.9 MeV protons or 27.6 MeV alpha particles incidented on one of the samples. The scattered ions from the sample were measured with a silicon surface detector of 500 microns depletion depth. The detector was hanged under a turntable at 150 mm apart from the target. The glancing angle of the detector to the incident beam direction could be changed. Fig 1 shows spectra of the scattered ions for the glancing angle of 150°, 120° and 105°. The sample was composed of a 12 micron mylar film and a 24 micron mylar film. A 2000 angstroms golden foil was sandwiched between these two films. The large hill in the spectrum shows the elastically scattered protons from the carbon atoms in the mylar foils, and a dip at the upper part of the hill shows a lack of carbon atoms at the place where the carbon atoms were exchanged with the golden atoms. The small peak of the elastically scattered protons from the oxygen atoms in the sample is seen adjacent the higher energy side of the carbon hill. Comparing the spectra at the different glancing angles, one can distinguish that the energy loss of the scattered protons, are less at the deeper backscattering angle. As the energy straggling of the scattered protons come to be larger with increasing of the total energy loss in the sample, the dip on the carbon hill can no more be distinguishable at the 105° scattering angle.

The RBS method could be applied to the quantitative analysis of constituents of chemical substance. A sample of ammonium citrate, $(\text{C}_6\text{H}_5\text{O}_7[\text{NH}_4])_3$, of 50 micrograms weight was spread out on a thin copper foil in area of 2cm^2 . In the spectrum of scattered protons, Fig. 2, three peaks which corresponded to carbon, nitrogen and oxygen were observed, As the elastic scattering cross section of protons were different for each element, the height of each peak did not correspond to the elemental ratio of

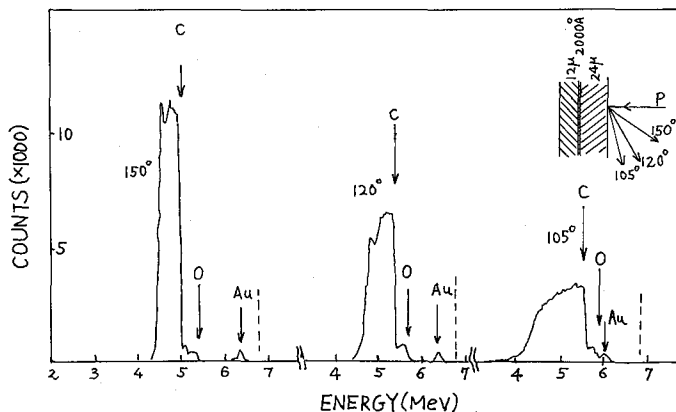


Fig. 1. 6.9 MeV proton backscattering spectrum observed at 150°, 120° and 105° from a 12 μ mylar-2000A gold-24 μ mylar "sandwich" target.

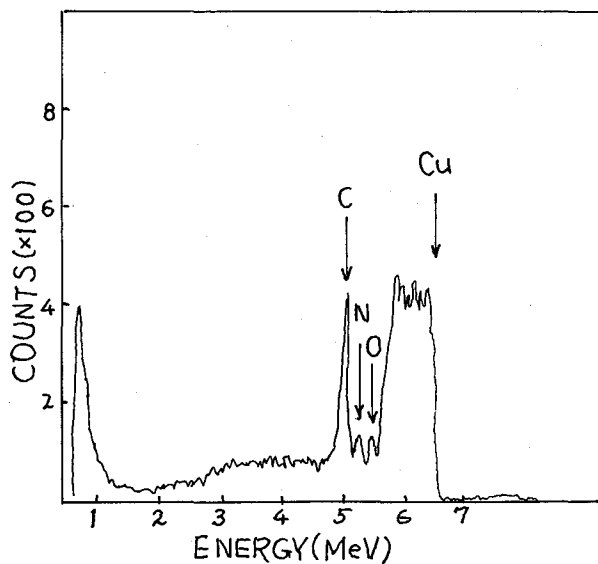


Fig. 2. 6.9 MeV proton backscattering spectrum observed at 150° from ammonium citrate of 50 μ g weight, 2cm² area on a copper foil.

the sample. However the elemental ratio could be easily obtained by the comparison with the spectrum of the sample of known elemental ratio. The elemental ratio of hydrogen atom in the sample also could be obtained when the forwardly scattered protons were observed.

In RBS analysis the measurements of one sample needed of only a few minutes, and the elemental ratio of the sample of 10¹⁵ molecules/cm² could be decided. About the local distribution of light elements in the sample surface, the resolution of about one micron was obtained at the depth of 20 microns.

In the case of RBS with alpha-particle the peaks in the spectra were not so clear as those in the proton spectra. The reason for this was the nuclear cross sections

came to be large at 27.6 MeV, and the secondary particles, such as inelastically scattered alpha particles and other particles which were generated by nuclear reactions raised the background counting in the spectra.

In conclusion the RBS method using the cyclotron could be used for the elemental analysis of a very small amount of the sample, and for the determination of the local distribution of light elements near the sample surface.

2. PIXE analysis

The proton induced X-ray emission (PIXE) analysis have been widely used in the trace element detection, since it can measure many elements simultaneously and nondestructively, and it requires very small amounts of sample.

The PIXE analysis was carried out with the Kyoto University Cyclotron^{5,6,7}. Fig. 3 shows the experimental set up of the experiments. To attain the highest sensitivity, the energy of the proton beam from the cyclotron was reduced from 6 MeV to 2-3 MeV by passing through an aluminum foil. Samples were mounted in a plastic chamber filled of helium gas at the atmospheric pressure. At this gas condition the sample exchanging process was simple, and the damage of the sample surface caused by beam bombarding were much restrained. A pure-germanium X-ray detector was placed at 130° direction to the proton beam, where the backwardly induced X-ray could be detected.

Application of the PIXE analysis to the ecological, biological and archaeological problems were performed with the Kyoto University Cyclotron.

For the study of the air pollution, atmospheric aerosol was analysed⁵. Aerosol were collected on paper filters. In most cases elements, Ca, Ti, Mn, Fe, Cu, Zn, and Pb, were detected. The correlation between the air pollution and the amounts of these elements were obviously observed.

Leaves of ginkgo trees at town streets were measured for the same problems⁵. Leaves were washed, rinsed and dried, and then were bombarded with the 3-MeV proton beam directory. Elements K, Ca, Mn, Fe, Cu and St were detected. The high concentration of Fe was observed for the sample from trees in polluted sites. However notable difference of the concentrations of K and Ca were not observed

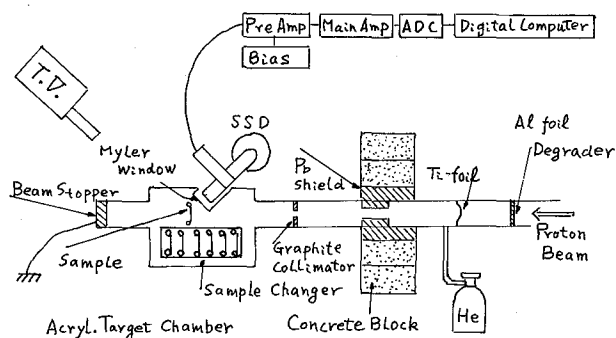


Fig. 3. Experimental set up of PIXE analysis by external beam method.

between samples. It was concluded that PIXE data about aerosol and ginkgo leaf showed the good measure for the local air pollution.

The application of the PIXE analysis to the historical change of the environment was studied⁹⁾. In annual rings of trees this information might be recorded. The pieces of wood from different annual rings, which grew in the period from 1948 to 1976, were ashed and dissolved in hot HNO_3 solution. In each solution Y_2O_3 was added as an internal standard material. The solution was spread on a thin mylar film. Elements, Ca, Ti, Cu, Zn, Mn, Sr, Ni and Pb, were detected. Notable increases of Mn and Sr were observed in the rings grown in the recent year. The reason for the annual change of concentration of elements could not be made clear.

Agricultural medicines remaining on rinds of fruits were easily detected by the PIXE analysis⁹⁾. The rinds of fruits were bombarded with the proton beam. High concentrations of Cu and Zn were observed on some rinds. These elements probably came from the agricultural medicine, like CuSO_4 and ZnSO_4 .

The trace elements in human hairs were easily analyzed by PIXE. Hairs were bombarded directly with the proton beam⁹⁾. The high concentrations of Pb and As were detected in some personal hairs.

The elemental analysis of tissue was important for the cancer study⁹⁾. Tissue slices of tumor, organ and musculin were analyzed by PIXE. The results were complicated and more extensive study was necessary to get the clear results about this subject.

Old objects of art and archaeological things were nondestructively examined by PIXE analysis⁹⁾. For example the composition of paint on an old picture and that of porcelain glaze were analyzed. Photo 3 is a photograph of an old picture and Fig. 4 shows the x-ray spectra of red, gold and green colors. The red color probably contained HgS and Pb_3O_4 , the golden color contained brass, and the green color contained $\text{Cu}_3(\text{AsO}_3)_2$. The proton irradiation time was about five seconds for taking one X-ray spectrum, and the picture was scarcely damaged by the proton bombardment.

Analysis of trace elements in water was important for monitoring the environmental pollution. The process of measurements had to be simple and easy. The PIXE analysis fulfilled this condition⁷⁾. To get the higher detection sensitivity ion exchange filters were used for concentration of trace elements in water. Expapier- F_2 ion filters were obtained from Sumitomo Chemical Industry. The filters were made of fibers which contained chelating minodiacetate functional groups. Since the chelating filter worked optimally in the neutral pH range, the additional pH adjustment which might introduce contamination to the sample was not required for natural water samples. This filter collected heavy metal ions more selectively than the usual acid ion-exchange resin when alkali and alkaline-earth ions were present. The internal standard material was added to the water sample and the sample was filtered by the filter paper. The filter paper was bombarded directly with the proton beam. The detection limits of metals in the solution were shown in Table 1. Fig. 5 shows the spectrum for the 100 ml of city water.

The method was tried for alcoholic drinks and fruit juices⁷⁾. The spectrum of



Photo. 3. Antique picture.

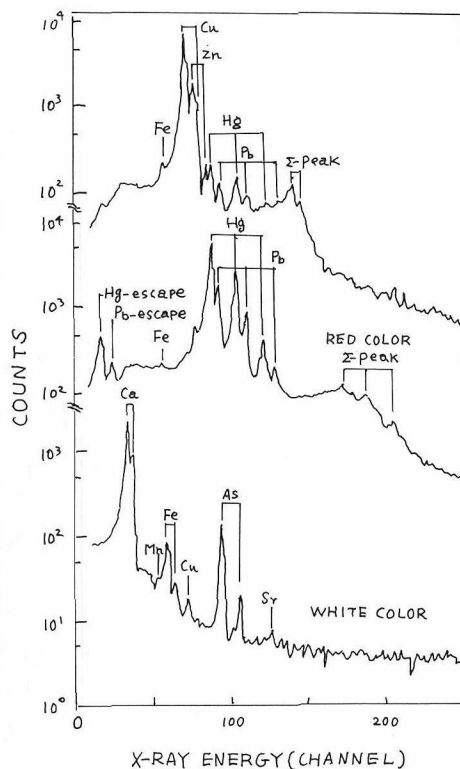


Fig. 4. X-ray spectrum from white color, red color and golden color painted on an antique picture by bombardment with 3 MeV protons.

Table 1. Lowest detection limit of metals in solution. irradiation time was 15 minutes.

element	atomic number	limit (μg)	element	atomic number	limit (μg)
Ti	22	0.1	Sr	38	5
Mn	25	1	Ag	47	25
Fe	26	0.1	Cd	48	25
Co	27	1	Sn	50	50
Ni	28	5	Hg	80	25
Cu	29	0.5	Pb	82	5
Zn	30	0.5			

rose wine was shown in Fig. 6.

RADIOBIOLOGY

1. Basic study about neutron therapy

Recently the trial neutron radiotherapy with the cyclotron have been undertaken

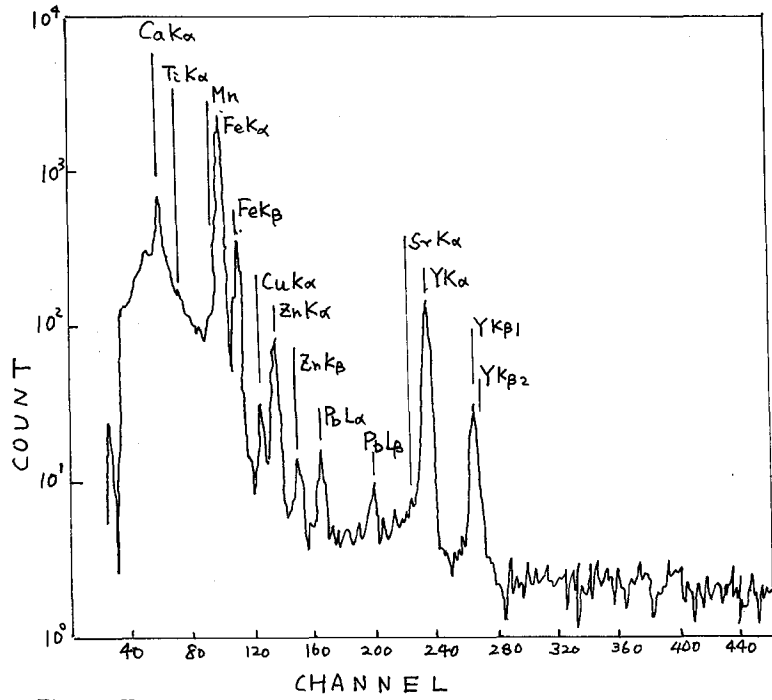


Fig. 5. X-ray spectrum of expapier-f₂ filters passed through drinking water of 100cc by bombardment with 4.2 MeV protons.

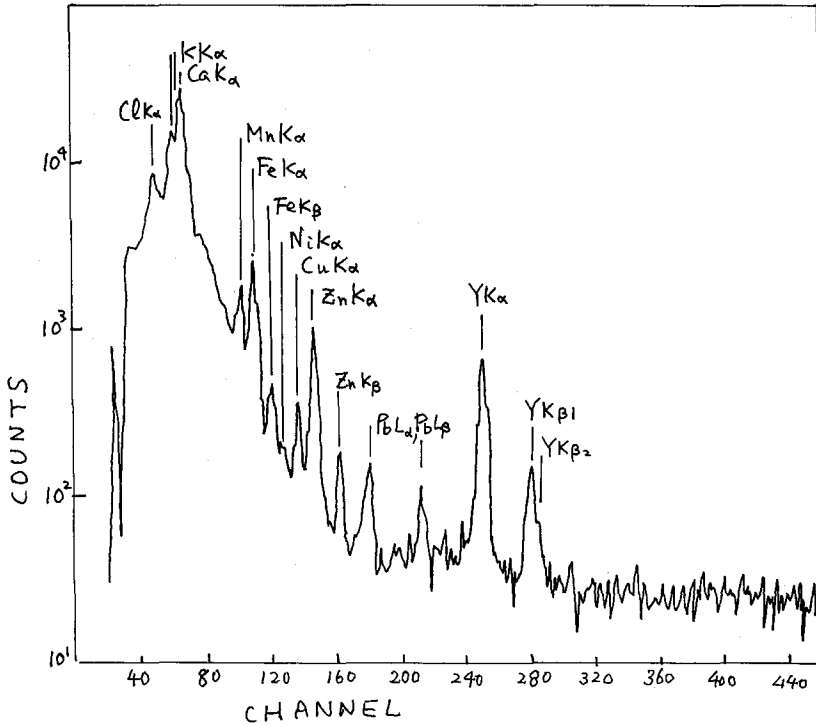


Fig. 6. X-ray spectrum of rose wine of 100cc. Experimental condition was same as Fig. 5.

at some hospitals in the world. Radiobiological advantages of the fast neutron radiotherapy have been thought as follows. Fast neutron has the high RBE (relative radiobiological effectiveness) value compared with X-rays, γ -rays and electrons. The recovery of tumorous cell from the lesions caused by the neutron irradiation is hindered compared with those caused by other irradiations. The OER (oxygen enhancement ratio) value of fast neutron is lower than other radiations. The clinical trial of fast neutron therapy should be performed under following conditions. The 50% depth-dose for a 5cm by 5cm irradiation field should occur 10cm deeper from the skin. And the dose rate should exceed 0.1 Gy/min (Gy=joule/kg) at the tumorous tissue. To satisfy the above conditions, the neutron energy must exceed about 14 MeV. The accelerator which can accelerate protons or deuterons of several tens-microampere beam current to the energy of higher than 20 MeV should be needed for the fast neutron generation. So the clinical trial of fast neutron therapy is currently limited by the availability of suitable neutron sources.

Although the Kyoto University Cyclotron did not fulfill the above conditions, the basic study about the neutron therapy was performed with the Kyoto University Cyclotron⁹⁾ Fast neutrons were generated by the deuteron bombardment of a thick beryllium target which was water-cooled and placed at the beam exit of the cyclotron. The energy of deuterons was 14 MeV and the beam current was few microamperes at the target. The forwardly generated neutrons passed through a thin flat ionization chamber, and the intensity of the neutron beam was monitored by this ionization chamber. The neutron beam was collimated to the size of 4cm by 6cm cross section by an iron shield of 30cm thickness and a paraffin-boron shield of 10cm thickness. The energy spectrum of the neutron was evaluated from the data of neutron TOF experiment and also from the data of other experiments. The energy of intensity maximum was about 6 MeV. The absorbed dose were measured with two cylindrical ionization chambers shown in Fig. 7. One chamber was constructed of tissue equivalent (TE) plastic and was filled of TE gas. Other had an approximately same size of the TE chamber, but was constructed of carbon or aluminum and was filled of argon or air. The TE chamber was used to determine the total absorbed dose in tissue and the carbon or aluminum chamber was used to determine the γ -ray component of the total absorbed dose. The responses of these chambers to γ -rays were calibrated in the standard radiation field of Cs-137 γ -rays. The absorbed dose due to neutrons and γ -rays at the n- γ mixed field produced with the cyclotron were obtained from the data of these two chambers. The ratio of the γ -ray component to the neutron component was 0.30 ± 0.02 and the average dose rate was about 0.06 Gy/min at the 0.48m SSD (source to skin distance).

The RBE value of the fast neutron beam was studied with the Kyoto University Cyclotron by a group of Professor Abe of the Kyoto University hospital⁹⁾. Effects of fast neutrons from the Kyoto University Cyclotron on a spontaneous C3H/He mouse mammary carcinoma were studied *in vivo*⁹⁾ As shown in Fig. 8 relative effectiveness of fast neutron beams (5~6rads/min) vs, Co-60 γ -ray, Cs-137 γ -rays and 32 MeV electron beam on 1 to 20 growth delay-days were changed with the growth delay-time and the dose rates of compared radiations. The values were reduced continuously 5.0

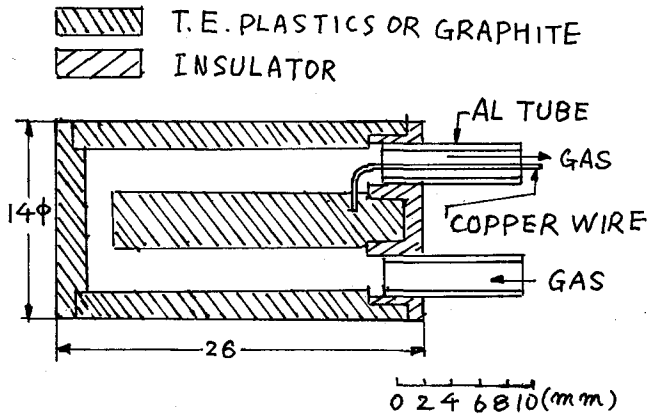


Fig. 7. Cross section of ionization chamber, TEP-TEG or C-air chamber.

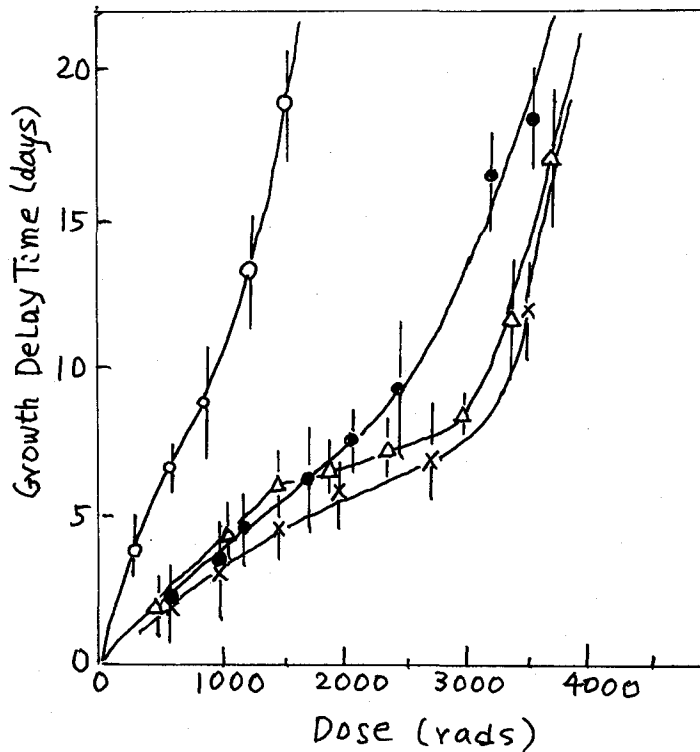


Fig. 8. Dose response curves on the growth delay-time for C30/He mouse mammary carcinoma, irradiated with $n+\gamma$ mixed (7~8rads/min, ○), 32 MeV electron beams (1500rads/min, ●), ^{60}Co γ -rays (150rads/min, Δ), and ^{137}Cs γ rays (15rads/min, ×).

to 3.0 as compared with ^{137}Cs γ -ray (15rads/min) and from 4.2 to 2.7 as compared with 32 MeV electron beam (1,500rads/min), however, the values as compared with ^{60}Co γ -rays (150rads/min) were smaller than those compared with 32 MeV electron

beam on 1 to 6 growth delay-days, and were similar to those for Cs-137 γ -rays on 8 to 20 growth delay-days.

2. Dose-effect relationship of chromosome aberrations induced by monoenergetic charged particles.

Recently an increasing amount of interest has been directed toward the investigation of the microstructure of energy deposition and its involvement in the formation of chromosome aberrations by radiations at the submicroscopic level. Monoenergetic charged particles are very useful for such detailed insights into the mechanism of chromosome aberration formation since they have a narrow distribution of LET (linear energy transformation) whereas photons and neutrons generate charged particles with a wide range of LET values.

The chromosome analysis in human peripheral blood lymphocytes exposed *in vitro* to monoenergetic 4.9 MeV protons and 23 MeV alpha particles generated by the Kyoto University Cyclotron was studied^{10,11}. And also the influence of magnetic field on the cytogenetic effect was investigated¹². The dose-response relationship of dicentrics and the distribution of these aberrations among cells were discussed in relation to the microscopic structure of energy deposition and the limitation of the interaction distance over which two lesions could combine to form dicentrics^{10,11}. Peripheral blood lymphocytes obtained from a healthy adult donor were irradiated by protons and alpha particles with the Kyoto University Cyclotron. A single layer of unstimulated G₀ lymphocytes was irradiated by a parallel beam of 4.9 MeV protons or 23 MeV alpha particles. Fluencies and kinetic energies were determined using a silicon semiconductor detector and an ionization chamber. The beam uniformity was checked and it was within 5% over the sample. The irradiated cells were immediately suspended in culture medium which consisted of RPMI-1640 supplemented with 20% foetal bovine serum, 4% PHA (phytohaemagglutinin) and 400units/ml penicillin, and then incubated at 37°C for 50 hours, of which the final 6 hours were in the presence of colcemid (0.5 μ g/ml). The cells were then processed for the chromosome preparation according to the standard air-drying method. With the culture method applied in this study, less than 3% of cells were in the second mitosis (ascertained by harlequin-staining) in sham-irradiated cultures.

Dicentric chromosomes were scored, and the observed yields of dicentrics among cells are given in the Fig. 9. The dose-response relationship were fitted to the linear quadratic model, $\mu = \alpha D + \beta D^2$, where μ is the dicentric yield and D is the dose in Gy.

The regression coefficients, α_p and β_p for protons and α_α and β_α for alpha particles were obtained as followings,

$$\alpha_p = (2.76 \pm 0.46) \times 10^{-1}, \beta_p = (1.36 \pm 0.28) \times 10^{-1},$$

$$\alpha_\alpha = (7.55 \pm 0.96) \times 10^{-1}, \beta_\alpha = (2.1 \pm 4.8) \times 10^{-1}.$$

As the standard error of β_α is large, the β_α is not significantly different from zero. The dose-reponse relation was not incompatible with a linear model, $\mu = \alpha_\alpha D$, which is more commonly applied to high LET radiations. The ratio of α_α to α_p was 2.74 ± 0.57 , which was considerably smaller than that expected from the LET ratio, $LET_\alpha / LET_p = 3.75$, suggesting the presence of LET dependent modification of the α coefficient.

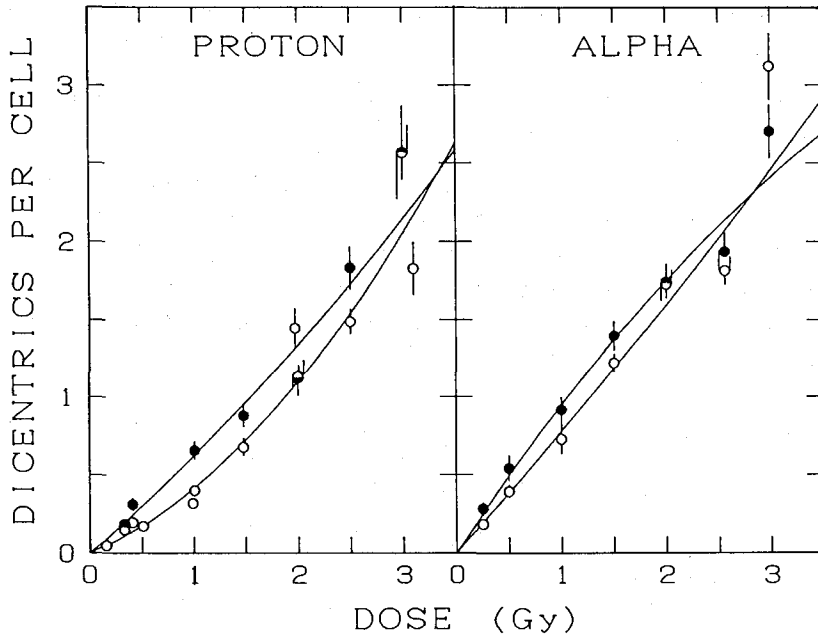


Fig. 9. Frequency of dicentric chromosomes plotted against proton dose, and alpha dose. Bar indicates standard error of mean. Solid line is a linear-quadratic regression curve fitted to data. Open circles: irradiation in the absence of magnetic field, closed circles: irradiation in magnetic field.

cient. Such discordance between the α ratio and the LET ratio seems to be a general property of the high LET radiation.

In the case of high LET radiations, because of the wide variation in the amount of energy imparted to a cell nucleus, the dose-response relation may be modified by selective removal of cell with more damage. Cells receiving more hits will be more likely to die, and such selective removal of cells implies that the cells observed at mitosis will have received, on average, less than the nominal amount of exposure, resulting in a distortion of the dose-response relationship. However, it should be noted that with high LET radiation the selective removal of cells with more damage may not be the only factor that can modify the dose-response relationship. Saturation of dicentric formation may be constituted another factor, in which the formation of dicentric chromosomes is interfered with by interaction of sublesions with those which have already interacted with other sublesions. Such negative interactions are expected to be more pronounced for radiations with higher LET.

In order to evaluate the distribution of dicentric chromosomes among cells, the relative variance (variance/mean, σ^2/μ) at each dose point was calculated. Fig. 10 shows the relative variances of the intercellular distributions of dicentric chromosomes. The relative variances for alpha particles were greater than those for protons and increased with the increase of the mean dicentric yield. The relative variances corresponding to various interaction distances were compared with observed values and a distance of around $0.2\mu\text{m}$ could best explain the data for the proton irradiation. Assuming that the

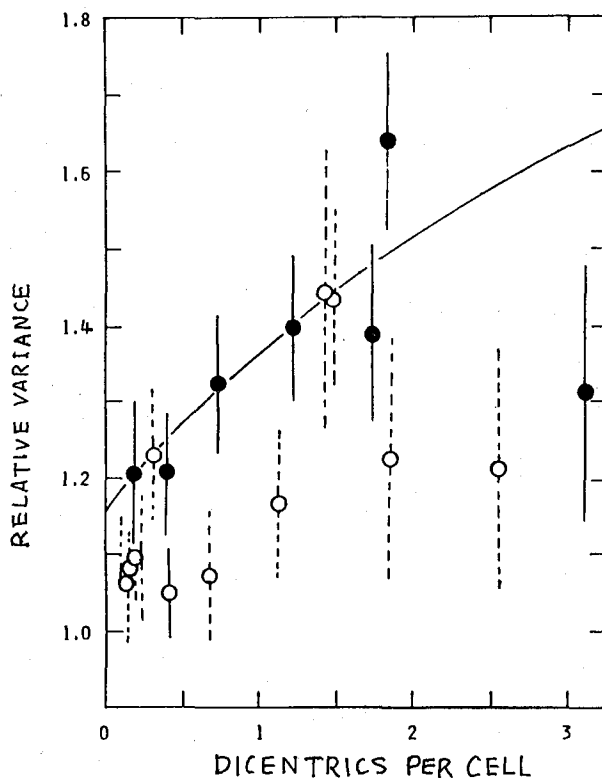


Fig. 10. Relative variances of the distribution of dicentrics plotted against the mean dicentric yield. Bar indicates the standard error, closed circles: 23 MeV alpha particles, Open circles: 4.9 MeV protons, a line represents an expected value assuming an interaction distance of $0.2\mu\text{m}$ and $\beta_{\alpha}=6.6\times 10^{-2}$.

probability of survival after alpha particles tracks was close to unity and the interaction distance was $0.2\mu\text{m}$, the β_{α} value of 6.6×10^{-2} gave a best fit to the observed relative variance. For a given relative variance, the value of interaction distance and β were mutually related. Therefore, for a better understanding of the kinematic of chromosome aberration formation, more precise estimates of interaction distance of β component should be thought. However, in any cases, the change in the relative variance associated with the change in mean dicentric yield can not be explained when $\beta=0$. Observation of the increase in the relative variance with increase in the mean dicentric yield suggests the presence of a significant amount of dose-quadratic component even for high LET radiations. Such a dose-quadratic component might be liable to be masked by the predominating linear component and also to be reduced by the selective loss of cells with more damage, which has a larger influence on β than on α . In the low dose range, the relative variance is approximated by $\sigma^2/\mu=1+a$, where a is the linear contribution to the number of dicentrics per track and is proportional to α . The relative variance is thus independent of β but is a function of α , which is in

Table 2. Regression coefficients, α and β of a linear quadratic model, $Y = \alpha D + \beta D^2$.

Radiation	Coefficient	No magnetic field	Magnetic field (1.1 T)
4.9 MeV	α	$(2.76 \pm 0.46) \times 10^{-1}$	$(5.70 \pm 0.86) \times 10^{-1}$
proton	β	$(1.36 \pm 0.28) \times 10^{-1}$	$(4.8 \pm 4.7) \times 10^{-2}$
23 MeV	α	$(7.55 \pm 0.96) \times 10^{-1}$	1.020 ± 0.089
alpha	β	$(2.1 \pm 4.8) \times 10^{-2}$	$(-7.2 \pm 4.0) \times 10^{-2}$

turn a function of LET. Data at the low dose level are in good agreement with this model, the relative variances for alpha particles being higher than for protons.

The effects of combined radiation and magnetic field on the biological systems in mammalian cells are particularly interesting. The cellular response to radiation is a consequence of complex biophysical and chemical processes, and thus it seems likely that such response may be modified by the magnetic field. The magnetic field also alters the physical property of radiation. When high energy electrons are traversing in the magnetic field, they experience the Lorentz force and are forced to follow spiral paths describing helices whose axes are parallel to the magnetic field. In a sufficiently strong transverse magnetic field, the radius of the helix become shorter, thus the electrons mimic high LET radiations and modify biological effects of radiation.

The effect of a strong static magnetic field on the induction of chromosome aberration in human peripheral blood lymphocytes was studied in combination with the *in vitro* exposure to 4.9 MeV protons and 23 MeV alpha particles¹²⁾. An electromagnet was set up so that the magnetic field direction was parallel to the beam of protons or alpha particles. The beam passed through a hole penetrating a pole of an electromagnet along the axis. The intensity of magnetic flux density at the beam path where the sample was located was about 1.1 T (tesla). The coil of the electromagnet was cooled by water flow to prevent temperature raise at the sample holder.

Dicentric chromosomes were scored. The frequencies of dicentrics plotted against proton or alpha dose in the magnetic field were compared with those obtained in the experiments in which no magnetic field was applied but otherwise processed in the same way. As seen from Fig. 9, the data in the presence and absence of magnetic field, were quite comparable. But aberration frequencies in experiments with magnetic field generally showed somewhat higher values. The calculated regression coefficients α and β are presented in Table 2. It was evident that the higher yield of chromosome aberrations in the presence of magnetic field was mainly due to the increase in the one-track component (α term), suggesting an increase in LET. Therefore, the difference between two conditions was more pronounced in the low-dose range. The regression coefficients for proton were significantly different between the two conditions at 5% significance level. However, for irradiation with alpha, the difference was not significant. Distribution of dicentrics among cells

irradiated in the magnetic field was compared with that of in no magnetic field. No systematic difference was seen between these distributions.

REFERENCES

- (1) T. Yanabu, *Bull. Inst. Chem. Res., Kyoto Univ.*, **55**, 74 (1977)
- (2) K. Kimura, et al., *Bull Inst. Chem. Res., Kyoto Univ.*, **39**, 368 (1961)
- (3) Y. Uemura, et al., *Bull Inst. Chem. Res., Kyoto Univ.*, **52**, 87 (1974)
- (4) Y. Hayashi, et al., *Bull Inst. Chem. Res., Kyoto Univ.*, **56**, 11 (1978)
- (5) T. Igaki, et al., *Bull Inst. Chem. Res., Kyoto Univ.*, **58**, 11 (1980)
- (6) T. Igaki, et al., *Hoshasen Radiation*, **10**, 17 (1983)
- (7) T. Yamada, et al., *Bull Inst. Chem. Res., Kyoto Univ.*, **62**, 17 (1984)
- (8) J. Miyajima, et al., *Bull Inst. Chem. Res., Kyoto Univ.*, **57**, 147 (1979)
- (9) T. Nishidai, et al., *J. Jap. Soc. Cancer Ther.*, **14**, 10 (1979)
- (10) T. Takatuji, et al., *Int. J. Radiat. Biol.*, **44**, 553 (1983)
- (11) T. Takatuji, et al., *Int. J. Radiat. Biol.*, **45**, 2337 (1984)
- (12) T. Takatuji, et al., *Int. J. Radia. Res.*, **30**, 238 (1989)